A 4D Frequency-Planar IIR Filter and its Application to Light Field Processing

by Don Dansereau and Len Bruton

Dept. of Electrical and Computer Engineering,
University of Calgary, Alberta, Canada

ABSTRACT

A 4D frequency-planar filter is described, having a steady-state frequency response with a pass band that approximates that of a 4D plane. It is shown that a light field containing Lambertian surfaces with no occlusions may be selectively filtered for depth using such a filter. Examples are given showing the effectiveness of the filter in scenes with and without occlusions. A technique for effectively reducing the length of the transient response of the filter is also proposed and the effectiveness of this technique demonstrated.

1. INTRODUCTION

Image-based rendering has gained attention as a fast alternative to geometric model-based rendering. Light field rendering and its variants [1][2] seek to model a 4D subset of the more general 7D plenoptic function [3] associated with a scene. In this way, the set of light rays permeating a scene are represented, rather than the geometry of the objects within the scene.

The 7D plenoptic function describes the light rays in a scene as a function of position, orientation, spectral content, and time. This can be simplified to a 4D function by considering only the color of each ray as a function of its position and orientation in a static scene, and by constraining each ray to have the same value at every point along its direction of propagation. This disallows scenes in which the medium attenuates light as it propagates, and it fails to completely model the behavior of rays as they are occluded. These limitations are not an issue for scenes in clear air, and for which the camera is not allowed to move behind occluding objects.

The 4D light field typically parameterizes light rays using the two-plane parameterization (2PP), as depicted in Fig. 1. Each ray is described by its point of intersection with two reference planes: the *s,t* plane given by $z=0$, and the *u,v* plane which is parallel to the *s,t* plane at some positive depth $z=d$. A full light field may consist of multiple sets of such planes, though this paper will deal only with a single set of reference planes. Note also that each sample of a light field can be taken as a grayscale intensity, though extension to utilize color samples given as red, green and blue components is a simple matter of keeping one light field for each color channel, and repeating each operation accordingly.

This paper deals exclusively with 4D light fields, and so all signals will be assumed to be 4-dimensional. The continuous-domain light field will be denoted as $L_{cont}(s,t,u,v)$, and the discrete-domain version as $L(n_s,n_t,n_u,n_v)$, where $\boldsymbol{n}$ is the discrete domain index of the signal. The continuous Fourier transform of the light field will be denoted as $L_{freq}(\Omega_s,\Omega_t,\Omega_u,\Omega_v)$.

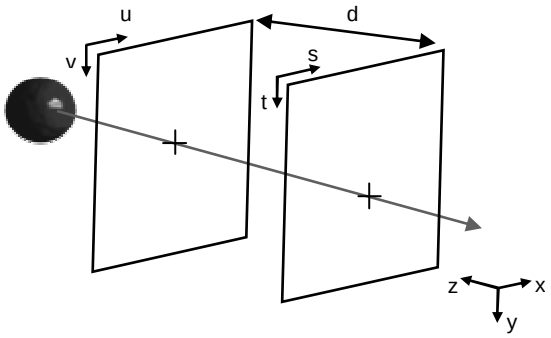

Figure 1. Two-plane parameterization of light rays.

This paper is organized as follows: Section 2 shows that a Lambertian scene can be filtered for depth using a 4D frequency-planar filter. Section 3 shows how to construct such a filter, including a technique for building a zero-phase version. Section 4 gives experimental results, and Section 5 discusses conclusions and indicates future work.

2. SPECTRAL CHARACTERISTICS OF LAMBERTIAN SCENES

2.1 The Omni-Directional Point Light Source

Fig. 2 depicts a 2D slice along *s* and *u* of a subset of the rays emanating from an omni-directional point source of light. It is clear from this figure that for any given point on the *s,t* plane there is only one point on the *u,v* plane for which a ray will intersect the light source. The result is that an *s,u* slice of the corresponding continuous-domain light field $L_{cont}(s,t,u,v)$ takes the form of a line, as depicted in Fig. 2b. The equation of this line is given by

$$(d/P_z - 1)\cdot s + u = P_x\, d/P_z \,, \tag{1}$$

where the point $\boldsymbol{P}$ gives the 3D position of the point light source, and d is the separation of the reference planes. The behavior in the *t and v* dimensions is similar, and can be expressed as

$$(d/P_z - 1)\cdot t + v = P_y\, d/P_z \,. \tag{2}$$

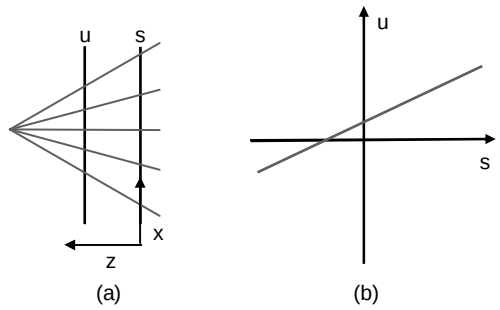

Figure 2. a) 2D slice of a point source of light shown with the two reference planes; b) 2D slice of the corresponding light field $L_{cont}(s,t,u,v)$.

In 4D space, (1) and (2) are the equations of two hyperplanes with normals in the directions $\boldsymbol{D_1}=[d/P_z\text{-}1,\ 0,1,0]$ and $\boldsymbol{D_2}=[0,d/P_z\text{-}1,0,1]$, respectively. The set of points which satisfies both (1) and (2) belongs to a plane defined by the intersection of these two hyperplanes. Only points belonging to this plane of intersection correspond to rays emanating from the point source – all other points in the light field will have a value of zero. Because the point source is omni-directional, every point in the plane will have the same value – equal to the color of the point light source. Thus, an omni-directional point light source is a plane of constant value in the light field $L_{cont}(s,t,u,v)$, where the plane is the solution of (1) and (2).

The normals of the hyperplanes (1) and (2) depend only on the distance P_z of the light source from the s,t plane, implying that a set of omni-directional point sources at a single depth z exists as a set of parallel planes in the light field $L_{cont}(s,t,u,v)$, each with constant value. The region of support (ROS) of the Fourier transform of such parallel planes can be shown to be a single frequency-domain plane through the origin, given as the intersection of the two frequency-domain hyperplanes

$$\Omega_s + (1-d/P_z)\cdot\Omega_u = 0\text{ , and} \tag{3}$$

$$\Omega_t + (1-d/P_z)\cdot\Omega_v = 0\text{ .} \tag{4}$$

Thus, the frequency-domain region of support (ROS) of a collection of omni-directional point sources at some depth $z=P_z$ is a single plane through the origin, where the plane is the solution of (3) and (4).

2.2 Lambertian Surfaces

A Lambertian surface is one which presents the same luminance independent of viewing angle [4], and thus behaves similarly to an omni-directional point light source. As a consequence, a Lambertian surface which exists at some constant depth $z=P_z$ will exist as a set of parallel planes in a light field, each of constant value, the frequency-domain ROS of which is a plane through the origin with an orientation which depends only on the z depth of the surface in the scene. This result is similar to that shown in Section 2.1 for a collection of omni-directional point light sources at a constant depth, and was also shown mathematically in [5].

Based on the above, we propose to design a filter to extract portions of a Lambertian scene at some depth by extracting the appropriately oriented plane in the frequency domain. Note that the frequency-planes at other orientations, corresponding to surfaces at other depths, all pass through the frequency-domain origin and thus intersect the planar passband of the filter at the origin. As a result, the low-frequency components of undesired signals (at stop band depths) will be transmitted. Note also that the filter functions with input scenes that do have occlusions and specular reflections. However, the desired occluded points in the input will assume values which depend on the value of the occluding surface, the desired specular reflections may vanish, and undesired specular reflections may interfere with desired surfaces.

3. 4D FREQUENCY-PLANAR FILTER

3.1 4D Frequency-Hyperplanar Filter

In order to construct a planar passband in 4D, two hyperplanar passbands, with appropriate orientations, are designed to intersect using the basic approach suggested in [6] for the 3D case. The design of the hyperplanar filters is a simple matter of extending the 3D frequency-planar filter presented in [6] by including an extra spatial variable. The input-output difference equation of the resulting filter is

$$y(\boldsymbol{n}) = \frac{1}{b_{0000}}\left[\begin{array}{l}\displaystyle\sum_{i=0}^{1}\sum_{j=0}^{1}\sum_{k=0}^{1}\sum_{l=0}^{1} L(n_s-i,n_t-j,n_u-k,n_v-l) - \\ \displaystyle\sum_{\substack{i=0\\ i+j+k+l\neq 0}}^{1}\sum_{j=0}^{1}\sum_{k=0}^{1}\sum_{l=0}^{1} b_{ijkl}\cdot y(n_s-i,n_t-j,n_u-k,n_v-l)\end{array}\right], \tag{5}$$

where the b_{ijkl} coefficients are found by iterating through the 16 sign configurations of $b_{ijkl} = 1+\left(\pm N_v \pm N_u \pm N_t \pm N_s\right)/B$, with $\boldsymbol{N}$ as the normal of the passband hyperplane, and with B as the -3dB bandwidth of the filter. The continuous-domain Laplace transform transfer function of the proposed filter is given as

$$T(s_s,s_t,s_u,s_v) = \frac{1}{1+(N_s s_s + N_t s_t + N_u s_u + N_v s_v)/B}\text{ ,} \tag{6}$$

which approximates a hyperplanar passband with its normal given by $\boldsymbol{N}$. This filter is practical-BIBO stable, but only for values of $\boldsymbol{N}$ which are positive along all 4 dimensions. In order to filter outside the first hexadecimant, the direction of iteration is reversed for all dimensions along which the normal is initially negative, then the sign of the normal is changed to be positive along those dimensions [6].

3.2 4D Frequency-Planar Filter

In order to construct the frequency-planar filter, two of the above frequency-hyperplanar filters are arranged in a cascaded configuration. The normal of each filter is selected to satisfy (3) and (4), respectively, resulting in the unit normals

$$\boldsymbol{N_1} = \frac{[1,0,1-d/P_z,0]}{\sqrt{1+(1-d/P_z)^2}} \text{ , and } \boldsymbol{N_2} = \frac{[0,1,0,1-d/P_z]}{\sqrt{1+(1-d/P_z)^2}} \text{ .} \quad (7)$$

The overall transfer function is given by

$$T(s_s,s_t,s_u,s_v) = T_1(s_s,s_t,s_u,s_v) \cdot T_2(s_s,s_t,s_u,s_v) \text{ ,} \quad (8)$$

where T_1 and T_2 are the transfer functions of the filters with normals $\boldsymbol{N_1}$ and $\boldsymbol{N_2}$, respectively. The magnitude frequency response of (8) is unity only where both filters have a magnitude frequency response of unity – that is, only where equations (3) and (4) are both satisfied. Thus, a filter that approximates a frequency-planar passband in 4D has been designed. The bandwidth of this filter is adjusted with B, and the orientation of the plane is adjusted to extract objects at a given depth in the light field by selecting $\boldsymbol{N_1}$ and $\boldsymbol{N_2}$ using (7).

3.3 Zero-phase filtering

The filter described above yields good depth discrimination but with a long non-ideal transient response in the output light field, the effects of which are darkening of the light field at the edges, and smearing of the images in the direction of iteration. This is especially significant for light fields which have low sample rates in s and t – a typical light field might have only tens of samples in these dimensions – and so a way of reducing the effects of the transient response is desirable.

The proposed technique is to employ zero-phase filtering: that is, to re-filter in a second pass the output signal with the direction of iteration reversed along each dimension. This is equivalent to flipping the normal of the frequency-hyperplanar passband of each frequency-hyperplanar filter in the second pass. This has no effect on the magnitude frequency response of the second-pass filter, but enforces a zero-phase frequency response, leading to a much shorter transient response at the output of the second-pass filter. By keeping extra output data as they are smeared off the edge of the light field by the first-pass filter, then utilizing them with the second-pass filter, the darkening of the edges of the light field can also be reduced significantly. Furthermore, because a second-pass filter is being applied, the overall magnitude frequency response is squared. The disadvantages of this zero-phase filtering technique are increased processing time and increased memory requirements.

4. RESULTS

The frequency-planar filter designed in Section 3.2 was applied with a bandwidth of B=0.05 to two light fields with geometric parameters as summarized in Table 1. The first light field was constructed using a raytracer and does not contain occlusions, while the second was measured using a gantry system and does contain occlusions. Each scene was filtered twice: once to extract foreground objects, and once to extract background objects. The filtering operation took about 10 minutes on a Pentium IV running at 1.3 GHz. The zero-phase technique described in Section 3.3 was also applied to the second light field, increasing the memory requirements by a factor of about 1.7, and the processing time to about ½-hour.

Color channels	3	s,t size (cm)	45
s,t samples	32	u,v size (cm)	36
u,v samples	256	separation d (cm)	57

Table 1. Light field parameters.

The results for the first light field can be seen in Fig. 3. Parts (a) through (c) are slices through u and v for values of s and t near the center of the light field. It is clear from the figure that the filter successfully extracted the two triangles, which are parallel with the s,t plane at depths of 60 and 50 cm. The transient response of the filter can be seen for the foreground and background triangles, respectively, in (d). These images are projections of the plane in which a single point of the triangle exists onto the u and v dimensions. The startup transient lasts about 7 samples in each dimension for this bandwidth.

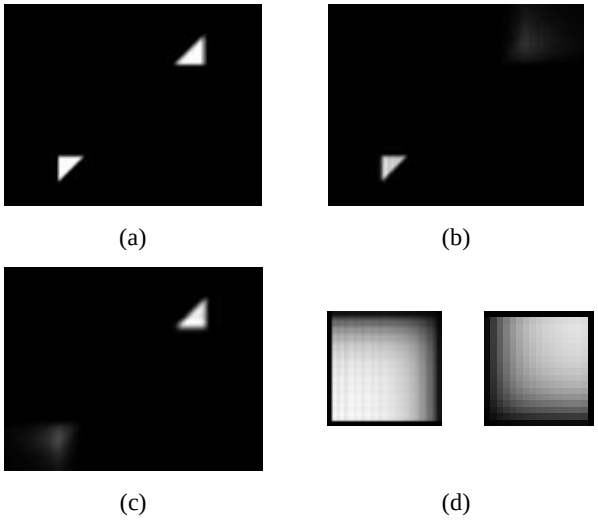

(a) (b) (c) (d)

Figure 3. Light field of raytraced scene with no occlusions. a) Unfiltered; b) Filtered for objects at 60 cm; c) Filtered for objects at 50 cm; d) Transient response as projected onto u,v.

The second light field, shown in Fig. 4, was acquired using a camera gantry. The background is a poster of a supernova imaged by the Dominion Radio Astrophysical Observatory in British Columbia, Canada. The foreground is a beer coaster – a wooden dowel can be seen holding the coaster in place. The poster and coaster are at depths of 66 and 48 cm, respectively. The filter was reasonably successful at extracting both objects, though the effects of the occlusion are clear near the center of the supernova in b), and the startup transient significantly darkens the edges of the images.

The effect of applying the zero-phase filtering technique described in Section 3.3 to the second light field is shown in Fig. 5. The startup transient is significantly reduced, as is most clearly seen near the top-right of both images. The selectivity has also noticeably increased, as the undesired portions of the images appear more blurred. The low-frequency components of the undesired signals remain, as anticipated.

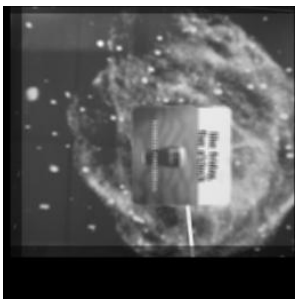

(a)

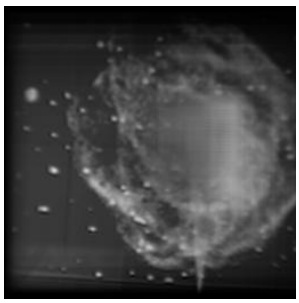

(b)

(c)

Figure 4. Measured scene with occlusions. a) Unfiltered; b) Filtered for objects at 66 cm; c) Filtered for objects at 48 cm.

(a)

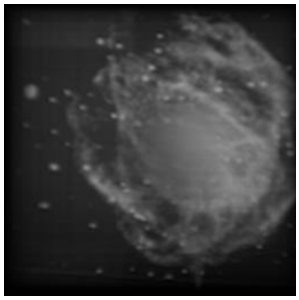

(b)

Figure 5. Measured light field filtered using zero-phase filter. a) Filtered for objects at 48 cm; b) Filtered for objects at 66 cm.

5. CONCLUSIONS AND FUTURE WORK

It has been shown that an omni-directional point source of light exists as a plane of constant intensity in a light field. As a result, a Lambertian surface at a constant depth in a scene has a frequency-domain ROS which is a plane through the origin. The construction of a 4D 1st-order frequency-planar recursive filter to extract this planar ROS was accomplished by intersecting two appropriately designed hyperplanar filters. The hyperplanar filters were constructed by extension of the method used to design a 3D frequency-planar filter. Finally, it was shown that zero-phase filtering can be accomplished by applying a second-pass filter with reversed directions of iteration.

The 4D planar filter was tested on two light fields – one created using raytracer output, and one measured using a gantry system. It was shown that the filter could successfully isolate elements at different depths. It was also shown that the proposed zero-phase technique significantly reduces the effects of the long transient response of the planar filter, while increasing selectivity, though at the cost of increased memory requirements and processing time.

Image-based techniques seem destined to become popular in processing and analysis applications such as object recognition [7], scene modeling [8], and robot navigation [9]. The possibility of applying simple techniques, such as the 1st-order filter presented in this paper, to accomplish complex tasks is exciting.

For future work, it should be possible to optimize the filter described in this paper significantly, increasing speed through parallelization, for example. A more thorough exploration of the impact of occlusions and specular reflection might also be interesting. Other possibilities include the exploration of non-linear techniques for processing light fields, possibly exploiting the correspondence between points in space and planes in light fields.

6. REFERENCES

[1] Levoy, M., and Hanrahan, P. "Light Field Rendering". *Proceedings SIGGRAPH '96*, 1996, pages 31-42.

[2] Gortler, S.J., Grzeszczuk, R., Szeliski, R., and Cohen, M. "The Lumigraph". *Proceedings SIGGRAPH '96*, 1996, pages 43-54.

[3] Adelson, E.H., and Bergen, J.R. "The Plenoptic Function and the Elements of Early Vision." *Computation Models of Visual Processing"*, 1991, pages 3-20.

[4] Hearn,Donald and M. Pauline Baker. *Computer Graphics, C version, 2nd Edition*, Prentice Hall, Inc, 1997.

[5] Chan, S.C., and Shum, H.Y. "A Spectral Analysis for Light Field Rendering". *Proceedings 2000 International Conference on Image Processing*, v 2, 2000, pages 25-28.

[6] Bruton, L.T., and Bartley, N.R. "Three-Dimensional Image Processing Using the Concept of Network Resonance". *IEEE Transactions on Circuits and Systems*, v CAS-32, n 7, Jul 1985, pages 664-672.

[7] Heigl, B., Denzler, J., and Niemann, H. "On the Application of Light Field Reconstruction for Statistical Object Recognition." *European Signal Processing Conference (EUSIPCO)*, 1998, pages 1101-1105.

[8] Vogelgsang, C., Heigl, B, Greiner, G., and Niemann, H. "Automatic Image-Based Scene Model Acquisition and Visualization". *Workshop Vision, Modeling and Visualization, Saarbrücken*, Germany, 2000, pages 189-198.

[9] Heigl, Denzler, and Niermann. "Combining Computer Graphics and Computer Vision for Probabilistic Visual Robot Navigation". *Enhanced and Synthetic Vision 2000*, volume 4023 of *Proceedings of SPIE*, April 2000, pages 226-235.